General Disclaimer

One or more of the Following Statements may affect this Document

- This document has been reproduced from the best copy furnished by the organizational source. It is being released in the interest of making available as much information as possible.

- This document may contain data, which exceeds the sheet parameters. It was furnished in this condition by the organizational source and is the best copy available.

- This document may contain tone-on-tone or color graphs, charts and/or pictures, which have been reproduced in black and white.

- This document is paginated as submitted by the original source.

- Portions of this document are not fully legible due to the historical nature of some of the material. However, it is the best reproduction available from the original submission.

Produced by the NASA Center for Aerospace Information (CASI)

NASA Contractor Report 167892

(NASA-CR-167892) MC CARBIDE STRUCTURES IN B(LC2)AR-M247 M.S. Thesis - Final Report (Purdue Univ.) 53 p HC A04/MF A01 CSCL 11F

N82-30374

Unclas
G3/26 28749

MC CARBIDE STRUCTURES IN Mar-M247

Stanley Walter Wawro

Purdue University
Lafayette, Indiana

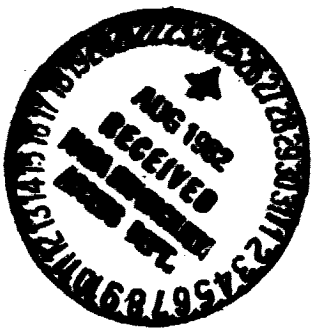

June 1982

Prepared for

NATIONAL AERONAUTICS AND SPACE ADMINISTRATION
Lewis Research Center
Under Grant NAG3-59

TABLE OF CONTENTS

INTRODUCTION

Nickel base superalloys were developed in the 1940's to meet the demands of the gas turbine industry for materials possessing high strength and oxidation resistance at elevated temperatures. A large number of alloy development advances have led to the creation of highly alloyed, microstructurally complex nickel base superalloys capable of operation at very high temperatures. One of the more recently developed nickel base superalloys is Mar-M247. Mar-M247 is used primarily for investment cast components of aircraft gas turbine engines. The nominal composition of Mar-M247 is given in Table I.

The basic microstructure of Mar-M247 consists of a highly alloyed austenitic matrix phase (γ) strengthened by a coherent precipitate phase (γ'). The γ phase is a random solid solution composed primarily of nickel, cobalt, chromium and tungsten. The γ' phase has an ordered fcc structure of the type A_3B, where the A atoms are primarily nickel and the B atoms are primarily aluminum and titanium. Most of the γ' forms by solid state precipitation; however, a small amount of γ' forms in structures known as "primary γ' islands." The primary γ' islands are formed from the last liquid to solidify. Primary γ' islands have a eutectic structure consisting of blocky γ' particles separated by layers of γ.

The other principal microconstituents found in Mar-M247 are MC carbides, which have the NaCl crystal structure. The metallic elements present in the MC carbides are titanium, tantalum, hafnium and tungsten.

Secondary carbides of the $M_{23}C_6$ type are sometimes present in the grain boundaries after heat treatment. $M_{23}C_6$ carbides have a complex cubic crystal structure; the metallic content is primarily chromium.

MC carbides in nickel base superalloys normally exist in the form of discrete particles with a "blocky" or equiaxed shape. Sometimes MC carbides assume a "Chinese script" morphology.[2-13] This script morphology consists of interconnected, rod shaped particles. It has been shown that such script carbides reduce ductility by providing easy paths for rapid crack propagation.[3]

Beginning in the late 1960's, hafnium was added to nickel base superalloys in amounts up to 2% by weight. Mar-M247 is one of these "hafnium-modified" superalloys. In general, the hafnium-modified superalloys possess greater ductility than conventional superalloys. The increased ductility is believed to be due largely to three microstructural effects:

1. Hafnium additions modify the MC carbide structure from a script morphology to a discrete, blocky morphology. (2,3,7-9,10)

2. Hafnium additions result in the formation of greater amounts of primary γ' islands. These primary γ' islands form mainly at the grain boundaries. The resulting grain boundary morphology is convoluted rather than planar.[3,11,12]

3. Hafnium additions prevent or reduce the formation of secondary carbides during heat treatment or elevated temperature service. Hafnium additions have been

found to convert the continuous grain boundary networks of $M_{23}C_6$ to discrete particles, while decreasing the total amount of $M_{23}C_6$ formed.[7,11] Hafnium additions also reduce the formation of Widmanstätten M_6C during elevated temperature exposure of alloys containing large amounts of Mo and W.[2]

Primary MC carbides form from the liquid during the initial solidification of nickel base superalloys. These alloys are remelted prior to casting of the final products. In the nickel base superalloys IN 100[4] and Inconel 713C,[5,6] it has been shown that not all of the MC carbides are dissolved during remelting. These undissolved carbides act as nucleation sites for further growth of MC carbides during subsequent solidification.[4,5,6] Thus, the presence of undissolved MC carbides in the liquid strongly influences the MC carbide structure of the final cast products. The term "carryover" is commonly used to refer to the phenomenon whereby such undissolved carbides exist in the final castings.

Studies by previous investigators have shown that several distinct types of MC carbides exist in Mar-M247.[2,12-14] The morphologies, chemical compositions and relative amounts of the various types of MC carbide depend on the thermal history of the material. One type of MC carbide found in these studies had a script morphology. These Ti-rich, script carbides had lower lattice parameters than the other MC carbides. The script MC carbides were most commonly found in the as-cast condition. The script carbides decomsed, either partially or totally, during long time exposures to

temperatures at or above 982°C. The decomposition of the script MC carbides was accompanied by the formation of discrete, Hf-rich MC carbides in or near the primary γ' islands.

The Hf-rich MC carbides formed during elevated temperature exposure are not believed to dissolve in the remelted liquid until temperatures greater than 1538°C are reached.[15] For reasons unrelated to the MC carbides, nickel base superalloys are normally remelted at temperatures below 1538°C. Thus, when Mar-M247 is remelted and cast after long time exposures in the range 982-1218°C, the Hf-rich MC carbides can be carried over to the final castings.[13]

The presence of script MC carbides in cast Mar-M247 products is regarded as undesirable due to the deleterious effects of such carbides on the ductility of the alloy. The conditions of formation of the script carbides are not well understood. Ti-rich script MC carbides have been found to exist in Mar-M247 ingot stock.[13] The presence of similar script MC carbides in products cast from such ingot stock has suggested the possibility of carryover during remelting and casting.[13]

This investigation was conducted to gain a better understanding of the MC carbides in Mar-M247. The particular objectives of this investigation were:

1. To characterize the relative amounts, distribution and morphologies of the MC carbides in several ingots produced from the same master heat at Mar-M247.
2. To determine if the MC carbide structure differed among the various ingots.

3. To characterize the MC carbide structure in several castings made from the remelted ingots.
4. To determine whether there was any carryover of the MC carbides from the ingots to the castings.

MATERIALS

The materials used in this investigation were provided by AiResearch Casting Company (ACC) of Torrance, California.

A. Remelt Ingots

Cross-sectional slices from each of 8 cylindrical remelt ingots were supplied by ACC. All of the ingots were from the same vacuum induction melted master heat. The master heat was composed totally of "virgin" material; no scrap was used. The ingots each weighed approximately 23 kg and were approximately 0.070 m in diameter. The lengths of the ingots were approximately 0.7 m. During the initial solidification of the ingots, a pipe had formed near the top of each ingot due to shrinkage. These pipes were backfilled with liquid metal from the same master heat. The ingots had been ground to remove surface defects.

From seven of the ingots, two slices, one from the top and one from the bottom, were provided. These slices were identified by the ingot number (1,15,30,45,60,75 or 91) from which they had been cut. The slices varied from 0.020 to 0.025 m in thickness.

A section from each slice had been removed by ACC to provide specimens for chemical analysis and metallographic observation. The results of these chemical analyses are given in Tables II and III.

From the remaining ingot, herein designated ingot number 99, three slices (top,middle, and bottom) were provided by ACC.

B. Castings

From each of the ingots numbered 1,15,30,45,60,75 and 91 ACC had poured two castings. The castings had been poured at a melt temperature of 1427°C. This melt temperature was not exceeded prior to casting. Sections of the gatings from each of these castings were provided by ACC. Each gating sample was identified by the remelt ingot number and whether it was from the first or second pour from that ingot. Each gating had a roughly square cross-section of 0.023 x 0.023 m; the lengths varied from 0.022 to 0.028 m. The chemical analyses of these gatings, provided by ACC, are given in Tables IV and V.

Four investment cast turbine blades were also provided by ACC. The blades were cast from one of the remelt ingots described above. The blades had been given a heat treatment of 16 hrs at 870°C, followed by air cooling.

EXPERIMENTAL PROCEDURES

A. Macrostructural Observation of the Ingot Slices

The cross-sectional faces of the ingot slices were ground through 600 grit silicon carbide paper. These slices were macroetched by immersion in Marbles' reagent for 1 to 2 minutes. (Marbles' reagent contains HCl, H_2O, and $CuSO_4$ in a 5:5:1 ratio; the HCl and H_2O are measured in milliliters, the $CuSO_4$ is measured in grams.) Each ingot slice was then cut on a plane 0.006 m from and parallel to its diameter. These new surfaces were similarly ground and macroetched. The macroetched surfaces were examined visually.

B. Selection of Specimens for Microstructural Analysis

Several small specimens were removed from each ingot slice for metallographic observation and electrolytic extraction of the carbide phases. These specimens were located at the center, edge, and selected intermediate distances from the center of each ingot slice. The radial distances of the intermediate specimens were kept constant for all of the ingots in order to allow comparison of the microstructures of the various ingots at equivalent positions. In most cases, the same specimen was used for carbide extraction after it had been observed metallographically.

Two specimens, one for metallography and one for carbide extraction, were removed from each gating sample. The specimens for metallography were cut in such a manner as to allow observation of one-half of the cross-sectional area of the gating. The specimens for carbide extraction were removed from the centers of the gatings. These specimens each measured approximately 0.005 x 0.005 x 0.01 m; the long dimension contained the axis of the gating.

Two adjacent specimens were removed from the thin airfoil section of each cast turbine blade. These specimens each measured approximately 0.020 x 0.008 x 0.002 m. The long dimension was parallel to the axis of the blade; the shortest dimension contained the full thickness of the blade. One of these specimens from each blade was used for metallography; the other was used for carbide extraction.

Two specimens, one for metallography and one for phase extraction, were removed from the root section of each cast turbine blade. The metallographic specimens were cut in such a manner as to allow observation of the entire cross-section of the root portion of each blade. The carbide extraction specimens from each blade were removed from the thickest portion of the blade root. No part of any carbide extraction specimen was closer than 0.003 m to the nearest edge of the blade root.

C. Optical Metallography

The specimens were ground and polished through 0.05 micron alumina. Metallographic observation of the specimens in the as-polished condition revealed the amounts and sizes of the carbides, but did not reveal other microstructural features. The specimens were subsequently

electropolished in a 20% H_2SO_4 in CH_3OH solution using a stainless steel beaker as the cathode. The electropolishing time was 5 sec, the applied potential was 20 volts. The specimens were etched by immersion for 20 sec in a 15% HCl in CH_3OH solution, to which a few drops of H_2O_2 were added. This preparation revealed the carbides as dark particles, the γ' as grey and the γ as white. The interdendritic regions appeared grey due to the increased amount of γ'.

D. Electrolytic Extraction of the Carbides

The carbide phases were separated from the matrix and γ' phases by a standard electrolytic extraction technique.[16] The current density was 700 A/m^2. One percent by weight of tartaric acid was added to the 10% HCl in CH_3OH electrolyte to prevent the formation of tungsten oxide. After the current was turned off, the carbides adhering to the undissolved portions of the specimens were removed by ultrasonic agitation. The residues were separated from the electrolyte by settling for at least 12 hrs, after which time the electrolyte was drawn off. The residues were rinsed with CH_3OH and allowed to settle again for 12 hrs. These rinsings were repeated several times. In some cases, multiple extractions from the same specimen were combined to increase the total amount of residue.

E. X-Ray Diffraction

The extracted residues were analyzed by X-ray powder diffraction to determine the phases present and their crystal structures. The residues, suspended in small amounts of CH_3OH, were applied to glass slides. The CH_3OH evaporated leaving dry residues that adhered to the

slides. X-ray diffraction patterns were recorded using a General Electric diffractometer. Nickel-filtered X-rays were generated by a copper tube operated at 40 kV and 19 ma. The diffractometer rotated at an angular (2θ) speed of 2^{o}/min, the chart recorder was operated at a speed of 0.0508 m/min. A 3° beam slit and a 0.2° dectector slit were used.

In some cases, the {200} peak of the low lattice parameter, script MC carbides was more intense than the {111} peak. This preferred orientation effect did not occur with the higher lattice parameter MC carbides, even when both types of carbides were present in the sample. This effect was eliminated by grinding the residues with an agate mortar and pestle prior to X-ray diffraction.

F. Scanning Electron Microscopy

For scanning electron microscopy, specimens were prepared by two methods:

1. For general microstructure, the specimens were electropolished and etched by methods similar to those used for optical microscopy. The electropolishing time was increased to 10 seconds and the etching time was increased to 30 seconds. When observed with the SEM, the carbides appeared as white or grey particles in relief, while the γ' appeared as dark, etched-out particles.

2. In order to clearly reveal the script morphology of the MC carbides, the specimens were electropolished for 100 seconds. The MC carbides were not attacked by this procedure and appeared as white particles in high relief against a black background.

G. Energy-Dispersive X-Ray Analysis

An EDAX 9100 energy dispersive X-ray analysis system attached to the SEM was used to obtain qualitative chemical analyses of the phases present. In situ analyses of the carbide phases were complicated by overlaps resulting from X-rays emitted by the adjacent matrix. For this reason chemical analyses were also done on the extracted carbides, which were placed on carbon stubs for SEM observation and analysis.

RESULTS

A. Structure of the Remelt Ingots

Each of the bottom slices of the remelt ingots contained an outer zone of columnar grains and an inner zone of equiaxed grains. The columnar grains extended approximately 0.012 m radially inward from the circumference of each slice. Columnar grains also extended 0.006 to 0.012 m along the length of each ingot from the extreme bottom edge.

The slice from the middle of ingot number 99 contained a zone of columnar grains extending 0.012 m radially inward from the circumference and a zone of equiaxed grains at the center. There was a small amount of shrinkage porosity at the very center of this slice.

Each of the top slices of the ingots contained four distinct macrostructural zones. Columnar grains extended approximately 0.012 m radially inward from the circumference. Adjacent to these columnar grains was a zone of equiaxed grains. A second zone of columnar grains was closer to the center of each top slice. At the very center of each top slice there was a second zone of equiaxed grains. Large amounts of shrinkage porosity existed at the centers and at the boundaries between the inner columnar and the outer equiaxed zones. The four-zone macrostructures resulted from backfilling the ingot pipes after initial solidification.

Several microstructural characteristics varied greatly with radial position within each ingot slice. These characteristics included MC carbide size, MC carbide morphology, the relative amounts of the different MC carbide types, and the spacing of the matrix dendrite arms. These variations indicated that the microstructural characteristics were determined largely by solidification conditions. In general, the more slowly solidified central portion of each ingot slice had a coarser microstructure than the rapidly solidified outer portions.

No significant microstructural differences were observed at equivalent locations among the eight ingots. For example, the microstructure at the center of any one bottom slice was indistinguishable from that at the center of any other bottom slice. The X-ray diffraction patterns of the carbides extracted from fixed locations from each of the ingots showed the same relative amounts of the different lattice parameter MC carbides. The only differences at equivalent locations occurred with the center and mid-radius locations of the top slices. At these locations, the solidification rate varied from ingot to ingot due to backfilling the different size pipes. This resulted in minor microstructural differences at equivalent locations.

The following paragraphs describe the microstructure of the center and edge specimens of the middle slice of ingot number 99. The microstructures of these specimens were representative of the extremes of solidification rate of the ingots. The microstructural characteristics of the other ingot specimens were intermediate between these extremes.

The MC carbides were located in the regions between the secondary dendrite arms. This interdendritic location was readily apparent at the slowly solidified centers of the ingots, as shown in Fig. 1a. At the more rapidly solidified edges of the ingots the secondary dendrite arm spacings were much smaller. Here too, the MC carbides were located interdendritically, although no satisfactory method was found to show this in micrographs. Figure 1b shows the carbide distribution typical of the edge specimens.

The total amount of MC carbide appeared to be constant throughout the ingots. Attempts were made to confirm this visual estimate by quantitative metallography using polished specimens. The small sizes and low volume fraction (less than 2%) of the MC carbides prevented reliable quantitative results from being obtained.

The MC carbide in the center specimen formed large script structures. Two such script structures are shown in Fig. 2a. The script structures consisted of elongated "arms" extending from central "cores." The central cores often appeared diamond-shaped when observed in planar section. Enlarged, blocky areas or "heads" were located on the ends of some of the script arms. These heads were usually located near grain boundaries or primary γ' islands. (The structures just to the right of the center of Fig. 2a are primary γ' islands.) Some of the MC carbide appeared as isolated particles. The isolated appearance was due to observation of the three-dimensional script structures in planar section.

When observed with the SEM, the conventionally electropolished and etched edge specimen appeared to contain discrete, angular or blocky

MC carbides, as shown in Fig. 2b. Long script arms, such as those observed in the center specimen, were not apparent.

The 100 second electropolishing preparation more clearly revealed the script structure of the MC carbides. The carbides that appeared isolated by more conventional metallographic preparations were seen to be connected in three-dimensional script structures when prepared by the deep electropolishing technique.

Figure 3a shows one such script MC carbide structure from the center specimen. Long primary arms extended at 90° angles from a faceted central core. Observations of other script structures showed that such arms extended in six mutually perpendicular directions from the cores. Secondary branches extended at approximately 90° angles from the primary arms. Some of these secondary branches contained tertiary branches, also at approximately 90° angles. A film-like region of MC carbide sometimes was located between the script arms, as shown at the right-hand side of Fig. 3a. Two of the enlarged, blocky heads of the MC carbide script structures are clearly visible at the left-hand side of Fig. 3a.

The MC carbides in the edge specimen formed smaller script structures, as shown in Fig. 3b. The central cores were smaller and less well developed than in the center specimen. The script arms were shorter than in the center specimen. A greater fraction of the total MC carbide existed in the form of heads in the edge specimen than in the center specimen.

In situ energy dispersive X-ray (EDX) analyses showed the MC carbides contained Ti, Ta, Hf, and W. The heads of the MC carbide

script structures contained greater amounts of Hf than the cores and arms. The transition from the low Hf to the high Hf regions of the script structures was abrupt. By placing the extracted carbide residues on carbon stubs, the EDX spectra were obtained with no contribution from the γ or γ' phases. Two representative EDX spectra are shown in Fig. 4. The spectrum shown in Fig. 4b is typical of the cores and arms of the script structures. In addition to Ta, Ti, Hf, and W, a small amount of Cr was present in the cores and arms. The spectrum shown in Fig. 4a is typical of the heads of the MC carbide script structures.

The X-ray diffraction peaks of the MC carbides were very broad, indicating variable composition. The profiles of the MC {200} diffraction peaks from the center and edge specimens are shown in Fig. 5. The lattice parameter of the MC carbide extracted from the center specimen was primarily 4.39 Å; the small shoulder on the low angle side of the main peak indicated the presence of a small amount of higher lattice parameter MC carbide. The lattice parameter of the MC carbide extracted from the edge specimen was primarily 4.50 Å, a significant amount of lower lattice parameter MC carbide was also present.

No secondary carbide phases ($M_{23}C_6$ or M_6C) were found in any of the ingot specimens.

B. Structure of the Castings

Each of the fourteen gating sections had a similar macrostructure. Columnar grains, oriented perpendicularly to the outer edges of the gatings extended approximately 0.007 m toward the centers. The grains at the centers of the gatings were equiaxed.

In each of the cast turbine blades, columnar grains extended from the edges to the center of the blades. Thus, each blade had a fully columnar microstructure.

The microstructures of each gating varied considerably with position within the gating. However, no microstructural differences were observed among the fourteen gatings at equivalent positions. There were no significant differences in the X-ray diffraction patterns of the extracted residues obtained from the different gatings. This indicated that the microstructure of a gating was determined neither by which remelted ingot the gating was cast from nor by whether the gating was cast from the first or second pour from a given ingot.

The microstructure of each blade varied considerably with position within the blade. However, similar microstructures were observed at similar positions within the different blades.

In general, the microstructural characteristics depended on the distance from the nearest edge of the castings. The microstructures of three specimens are described in the following paragraphs. These three specimens are:

1. The thin airfoil section of blade number 2. This specimen was 0.002 m thick. The micrographs were taken at the center of the specimen. The carbides were extracted from a specimen that included the full thickness of the airfoil section. The microstructure of this specimen was representative of the most rapidly solidified portions of the cast blades.

2. The center of the root section of blade number 2. The micrographs were taken at a distance of approximately 0.005 m from the nearest edge of the casting. No portion of the carbide extraction specimen was closer than 0.003 m to an edge of the casting. The microstructure of this specimen was representative of the most slowly solidified portions of the cast blades.
3. The center of the gating from the first pour of ingot number 45. The micrographs were taken at a distance of approximately 0.012 m from the nearest edge of the gating. No portion of the phase extraction specimen was closer than 0.009 m to an edge of the gating. The microstructure of this specimen was representative of the most slowly solidified portions of all of the remelted and cast material.

The MC carbides were located in the interdendritic regions of the castings. Figures 6a, 6b, and 7 show the microstructures of the airfoil, root and gating specimens, respectively. The MC carbides in these micrographs appeared as isolated particles. However, as in the remelt ingots, the isolated appearance of the MC carbide resulted from observing the script structures in planar section.

The total amount of MC carbide in the different cast specimens appeared constant. As with the ingot specimens, this visual estimate was not verified by quantitative methods.

The MC carbide formed large script structures in the gating specimen, as shown in Fig. 8. The script structures had long arms extending to the grain boundaries and primary γ' islands. The script arms sometimes followed the grain boundaries. A few of the arms terminated in enlarged heads at the primary γ' islands, as shown at the top and extreme left sides of Fig. 8.

The MC carbide script structures were smaller at the center of the blade root specimen than at the center of the gating. One of these script structures is shown in Fig. 9a. A small amount of $M_{23}C_6$ existed at the grain boundaries, as shown in Fig. 9b.

The MC carbide formed even smaller script structures in the airfoil specimen. One of these structures is shown in Fig. 10a. At the bottom of Fig. 10a are several MC particles that appear isolated; however, the deep electropolishing technique showed that such particles were connected. $M_{23}C_6$ was present at the grain boundaries and the outer edges of the primary γ' islands. This $M_{23}C_6$ formed as discrete, blocky or spheroidal particles, as shown in Fig. 10b. The amount of $M_{23}C_6$ in the airfoil specimen was much larger than in the root specimen. In both specimens the amount of MC carbide was many times larger than the amount of $M_{23}C_6$.

Figures 11a and 11b show typical MC carbide script structures from the gating and root specimens, respectively. The MC script structures of the gating were approximately twice as large as those of the roots. Both structures contained elongated arms extending outward from a

central, octahedral core. The cores of the gating script structure were several times larger than those of the root. The primary arms contained numerous branches at 90° angles. The script arms had serrated surfaces. Smooth, angular, slightly enlarged heads were located at the ends of some of the script arms.

The MC carbide script structures of the airfoil specimen are shown in Fig. 12 as observed after deep electropolishing. These script structures were smaller than those observed in the root or gating specimens. The script structure of the MC carbides in the airfoil specimens were different in several respects from the script structures of the ingots, roots or gatings. The cores of the script carbides did not possess the sharply defined, octahedral shape observed in the other specimens. No particular angular orientation of the script arms were observed. The script arms were very rarely branched. The serrated arms of the script carbides terminated in enlarged, smooth, angular heads.

Energy-dispersive X-ray analyses of the script carbides from the castings showed the script arms and cores contained Ti, Ta, Hf, W, and a small amount of Cr. The heads contained greater amounts of Hf and no Cr. The EDX spectra of the MC carbides from the cast specimens were very similar to those shown in Fig. 4, which were from the ingot specimens.

The $M_{23}C_6$ particles found in the root and airfoil specimens contained mostly Cr. A small amount of W was also present in the $M_{23}C_6$. The lattice parameter of the $M_{23}C_6$ carbide was 10.69 Å. No M_6C was found in any of the castings.

X-ray diffraction of the extracted carbide residues from the cast specimens revealed that the predominant MC carbide had a lattice parameter of 4.39 Å. A smaller amount of higher lattice parameter MC carbide was present in each of the specimens. The amount of this higher lattice parameter carbide was greatest in the airfoil specimens and least in the gating specimens. Diffraction profiles of the MC {200} peaks are shown in Fig. 13. A very small contribution to the profiles of the airfoil and root specimens was due to the $M_{23}C_6$ {422} peaks. This contribution was at 2θ angle of 41.4°, and was estimated to contribute no more than 10% of the total intensity.

DISCUSSION

All of the MC carbide present in both the ingots and castings existed as script structures. These MC carbide script structures were located in the regions between the secondary dendrite arms. Each of the script structures was composed of three characteristic parts:

1. A central core. The central cores of the MC carbide in the rapidly solidified portions of the cast turbine blades had irregular shapes. The central cores in all of the other material had sharply defined, octahedral shapes.
2. Elongated arms. The elongated arms of the script MC carbide structures extended outward from the central cores. In those script structures that possessed octahedral cores, primary script arms extended from the six corners of the core. Secondary and higher order arms branched from the script arms at 90° angles.
3. Blocky or angular heads. The heads of the script MC carbides were located at the ends of the script arms, in the vicinity of grain boundaries or primary γ' islands.

The script morphology of the MC carbides was not always apparent when the specimens were prepared by conventional metallographic techniques. The script morphology was only discerned when the

specimens were deeply etched, as with the 100 second electropolish used in this investigation. Another commonly used technique for studying the carbide structures in superalloys also obscured the true morphology of the MC carbides. When the extracted MC carbide residues were observed with the SEM, much of the carbide appeared to be discrete particles. These "discrete" particles were actually fragments of much larger script structures. During the preparation of the extracted carbides for SEM observation, most of the MC carbide script structures were somehow broken into small fragments.

The cores and arms of the script structures have the chemical composition (Ti, Cr, Hf, Ta, W)C. Ti and Ta are the major elements in the cores and arms; the amount of Cr is very small. The heads of the script structures have the composition (Ti, Hf, Ta, W)C. The amount of Hf in the heads is much greater than in the cores and arms.

It is common practice to write the formula of carbide phases with the NaCl crystal structure as MC. This does not necessarily indicate that a one-to-one stoichiometric relationship between the metal and carbon atoms. A significant fraction of the carbon atoms can be missing from the lattice. For example, in the MC carbide TiC_x, the carbon fraction can vary from $x \gtrsim 0.46$ to $x \gtrsim 0.988$.[17] Oxygen and nitrogen can substitute for some of the carbon in MC carbides.[18] No analyses of the nonmetallic elements in the MC carbides were done in this investigation. The use of the formula MC in this report does not preclude the possibilities of nonstoichiometry or of oxygen and nitrogen substitutions.

The amount of "head"-type MC carbide relative to the amount of "core and arm"-type varied with position within the samples. In general, the outer, more rapidly solidified portions of the ingots and castings contained greater relative amounts of "head"-type MC carbide. The X-ray diffraction studies showed greater amounts of high lattice parameter ($\approx$ 4.50 Å) MC carbide in the more rapidly solidified material. On this basis, it can be concluded that the lattice parameter of the "head"-type MC carbide is approximately 4.50 Å and that the lattice parameter of the "core and arm"-type MC carbide is approximately 4.39 Å.

The assignment of the 4.39 Å and 4.50 Å lattice parameters to the "core and arm"-type and the "head" type MC carbide is further supported by consideration of the effects of chemical composition on lattice parameter. The lattice parameters of TiC, TaC, and HfC are 4.329 Å, 4.456 Å, and 4.641 Å, respectively.[19] Tungsten does not form a cubic monocarbide; however, a theoretical lattice parameter of 4.32 Å has been calculated for hypothetical cubic WC based on extrapolation of data from the (Hf, W)C system.[20] The lattice parameter of $(Hf_x, Ti_{1-x})C$ increases almost linearly from the lattice parameter of TiC to that of HfC as the amount of Hf is increased from $x = 0$ to $x = 1$.[20] A similar effect probably occurs in the multicomponent MC carbides in Mar-M247. This lends additional support to the conclusion that the Hf-rich "head"-type MC carbides have a higher lattice parameter than the "core and arm"-type.

No carryover of the MC carbides from the ingots to the castings occurred. The following observations support this conclusion:

1. The MC carbide script structures were much smaller in the most rapidly solidified portions of the castings than in any portion of the ingots.
2. The shape of the MC carbides in the most rapidly solidified portions of the casting was different than the shape of the script carbides in the ingots. The script carbide arms in the rapidly solidified portions of the castings were not branched and the angles between the arms were not 90°.
3. The central cores of the MC carbide script structures in the airfoil sections had lower Hf contents than the heads of the carbides in the ingots.
4. The central cores of the MC carbides in the rapidly solidified portions of the castings were smaller than the heads of the script carbides in the ingots.
5. No isolated MC carbide particles existed in the castings, i.e., all of the MC carbide existed as parts of the script structures.

The first two of the above observations indicated that the low hafnium, core and arm portions of the MC carbide script structures were dissolved in the liquid at 1427°C. The last three observations indicated that the Hf-rich head portions were also dissolved.

The fact that the MC carbides did not carryover upon remelting at 1427°C does not preclude the possibility of carryover when Mar-M247 is remelted at lower temperatures. Similarly, the results of this investigation do not preclude the possibility of carryover of the very

high Hf, very high lattice parameter MC carbide that forms in Mar-M247 during long time exposures to temperatures greater than 980°C.[2,12-14]

CONCLUSIONS

1. All of the MC carbide formed in script morphologies in Mar-M247 when solidified under the conditions of this investigation.
2. No significant variations in the MC carbide amounts, compositions or morphologies existed at equivalent locations within the various ingots. The nature of the MC carbides was determined primarily by solidification conditions.
3. The MC carbide formed in the interdendritic regions during solidification of both the ingots and the castings.
4. All of the MC carbide that existed in the ingots was completely dissolved upon remelting at 1427°C.
5. The MC carbide script structures consisted of elongated arms extending from a central core. The script arms were often branched. The script arms often terminated with enlarged, blocky or angular heads near primary γ' islands or grain boundaries.
6. The cores and arms of the MC carbide script structures had lattice parameters of approximately 4.39 Å and compositions (Ti,Hf,Ta,W,Cr)C. Ti and Ta were the major metallic elements in the MC carbide cores and arms. The heads of the MC carbide script structures had lattice parameters of approximately 4.50 Å and compositions (Ti,Hf,Ta,W)C. The amount of Hf in the heads was much greater than in the cores and arms.

7. The size of the MC carbide script structures increased with decreased solidification rate. The small script structures contained relatively greater amounts of head-type MC carbide than the large script structures.

RECOMMENDATIONS FOR FURTHER STUDY

1. In order to determine the liquid temperatures at which MC carbides exist in the remelted alloy, rapid solidification experiments should be performed from an incremental series of temperatures above the liquidus. Techniques such as those used for producing metal powders or amorphous metals can provide the necessary high solidification rates. Some MC carbide might form during such rapid solidification. However, it is possible that any MC carbides that existed in the liquid prior to solidification would differ from the MC carbides formed during solidification. These differences would possibly include chemical composition, morphology and/or distribution.
2. Differential thermal analysis (DTA) experiments might provide information concerning the temperatures of formation (on cooling experiments) or dissolution (on heating) of the different MC carbide types. The DTA technique might not be sensitive enough due to the small amounts of MC carbide present in the alloy. Since the nature of the MC carbide appears to be determined by solidification parameters, proper selection of the cooling rates used in the DTA experiments will be important.
3. A unidirectional solidification technique, such as that used by Fernandez, et al.,[4] can be used to solidify Mar-M247 under controlled thermal gradients and growth rates. Metallographic

ORIGINAL PAGE IS
OF POOR QUALITY

examination of specimens solidified by this technique would permit correlations of carbide size and morphology with the solidification parameters.

4. Although it is widely believed that large script carbides have deleterious effects on the mechanical properties of Mar-M247, the effects of fine script carbides such as those found in the cast turbine blades have not been demonstrated. The mechanical properties of Mar-M247 solidified at various controlled rates should be determined. The sizes of the MC carbide script structures obtained from each solidification rate should also be measured to determine whether a correlation with mechanical properties exists.

ORIGINAL PAGE IS
OF POOR QUALITY

REFERENCES

1. High Temperature High Strength Nickel Base Alloys, 3rd Ed., p. 4, The International Nickel Company, New York, 1976.

2. J. F. Radavich, R. G. Riel, and C. Keene: Proceedings of the Third Annual Purdue University Student-Industry High Temperature Materials Seminar, School of Materials Engineering, Purdue University, West Lafayette, IN, 1975, pp. 84-97.

3. P. S. Kotval, J. D. Venables, and R. W. Calder: Met. Trans., 1972, 3, pp. 453-458.

4. R. Fernandez, J. C. Lecomte, and T. Z. Kattamis: Met. Trans., 1978, 9A, pp. 1381-1386.

5. A. K. Bhambri, T. Z. Kattamis, and J. E. Morral: Met. Trans., 1975, 6B, pp. 523-537.

6. S. C. Fegan, T. Z. Kattamis, A. K. Bhambri, and J. E. Morral: J. Mater. Sci., 1975, 10, pp. 1266-1270.

7. J. M. Dahl, W. F. Danesi, and R. G. Dunn: Met. Trans., 1973, 4, pp. 1087-1096.

8. J. D. Varin: In The Superalloys, C. T. Sims and W. C. Hagel, Eds., pp. 252-256, John Wiley and Sons, New York, 1972.

9. R. T. Holt and W. Wallace: Int. Met. Rev., 1976, 21, pp. 1-24.

10. C. J. Burton: Proceedings of the Third International Symposium on Superalloys, Clairtor's Publishing Division, Baton Rough, LA, 1976, pp. 147-157.

11. J. E. Doherty, B. H. Kear, and A. F. Giamei: J. Metals, 1971, 23, pp. 59-62.

12. C. Lund and J. F. Radavich: Proceedings of the Fourth International Symposium on Superalloys, American Society for Metals, Metals Park, OH, 1980, pp. 85-98.

13. J. F. Radavich: Purdue University, West Lafayette, IN, unpublished research.

ORIGINAL PAGE IS
OF POOR QUALITY

14. J. F. Radavich and M. A. Engel: Proceedings of the Fifth Annual Purdue University Student-Industry High Temperature Materials Seminar, School of Materials Engineering, Purdue University, West Lafayette, IN, 1979, pp. 140-151.

15. J. F. Radavich: Proceedings of the Fifth Annual Purdue University Student-Industry High Temperature Materials Seminar, School of Materials Engineering, Purdue University, West Lafayette, IN, 1979, pp. 152-153.

16. M. J. Donachie and O. H. Kriege: J. Mater., 1972, 7, pp. 269-278.

17. E. K. Storms: The Refractory Carbides, pp. 4-6, Academic Press, New York, 1967.

18. E. K. Storms: pp. 235-236.

19. JCPDS Powder Diffraction File, File Nos. 6-614, 12-1292, 9-368, JCPDS International Center for Diffraction Data, Swarthmore, PA.

20. P. Rogl, S. K. Naik, and E. Rudy: Monatsh. Chem., 1977, 108, pp. 1189-1211.

ORIGINAL PAGE IS
OF POOR QUALITY

TABLE I. Nominal Chemical Composition of Mar-M247.

Element	Weight Percent
Cr	8.2
Co	10.0
Mo	0.6
W	10.0
Ta	3.0
Al	5.5
Ti	1.0
C	0.16
B	0.015
Zr	0.09
Hf	1.5
Ni	Balance

Source: Reference #1.

TABLE II. Chemical Composition of Bottom Slices of Remelt Ingots.

(Weight Percent)

Element	Ingot Number 1	15	30	45	60	75	91
C	0.153	0.150	0.145	0.150	0.145	0.150	0.148
Mn	0.01	0.01	0.02	0.01	0.01	0.05	0.05
S	0.002	0.002	0.002	0.002	0.002	0.002	0.002
P	*	*	*	*	*	*	*
Si	0.05	0.05	0.05	0.05	0.05	0.05	0.05
Cr	8.38	8.35	8.30	8.33	8.35	8.26	8.27
Co	9.91	9.96	9.92	9.97	9.90	9.96	9.97
Mo	0.69	0.71	0.68	0.70	0.68	0.70	0.69
Ti	1.00	0.99	0.98	0.99	0.98	0.99	0.99
Al	5.57	5.60	5.53	5.58	5.55	5.50	5.51
Zr	0.055	0.055	0.060	0.060	0.055	0.05	0.05
B	0.014	0.013	0.013	0.013	0.014	0.013	0.013
Fe	0.09	0.09	0.10	0.10	0.09	0.04	0.04
W	9.97	10.02	9.97	10.00	9.98	9.99	9.96
Ta	2.97	2.95	2.97	2.93	2.93	2.96	2.94
Hf	1.45	1.43	1.48	1.45	1.43	1.48	1.45
Ni	Bal.	Bal.	Bal.	Bal.	Bal.	Bal.	Bal.

*not determined.

ORIGINAL PAGE IS
OF POOR QUALITY

TABLE III. Chemical Composition of Top Slices of Remelt Ingots.

(Weight Percent)

Element	Ingot Number 1	15	30	45	60	75	91
C	0.14	0.13	0.14	0.15	0.13	0.13	0.14
Mn	0.01	0.01	0.01	0.01	0.01	0.01	0.01
S	0.005	0.003	0.005	0.006	0.004	0.004	0.004
P	0.003	0.002	0.003	0.003	0.003	0.003	0.003
Si	0.01	0.01	0.01	0.01	0.01	0.01	0.01
Cr	8.30	8.03	8.25	8.04	8.05	8.10	8.05
Co	10.85	9.40	9.95	10.10	10.06	9.25	10.10
Mo	0.72	0.54	0.71	0.67	0.65	0.69	0.71
Ti	1.20	0.94	1.18	1.12	1.10	1.05	1.14
Al	5.42	5.38	5.37	5.37	5.35	5.43	5.30
Zr	0.041	0.040	0.041	0.041	0.041	0.041	0.049
B	0.014	0.012	0.013	0.013	0.013	0.012	0.013
Fe	0.06	0.04	0.06	0.05	0.05	0.05	0.05
W	9.71	9.77	9.69	9.85	9.74	9.72	9.87
Ta	2.99	2.96	2.86	2.81	2.89	2.86	2.93
Hf	1.59	1.58	1.58	1.59	1.59	1.60	1.58
Ni	Bal.	Bal.	Bal.	Bal.	Bal.	Bal.	Bal.

ORIGINAL PAGE IS
OF POOR QUALITY

TABLE IV. Chemical Composition of First Pour Castings

(Weight Percent)

Element	Ingot Number 1	15	30	45	60	75	91
C	0.14	0.13	0.13	0.14	0.14	0.14	0.13
Mn	*	*	*	*	*	*	*
S	<0.005	<0.005	<0.005	<0.005	<0.005	<0.005	<0.005
P	*	*	*	*	*	*	*
Si	0.03	0.02	0.02	0.03	0.03	0.02	0.03
Cr	8.39	8.36	8.46	8.52	8.55	8.51	8.41
Co	9.83	9.83	9.88	9.97	9.91	9.97	9.91
Mo	0.72	0.76	0.76	0.73	0.76	0.73	0.70
Ti	1.09	1.08	1.08	1.09	1.10	1.08	1.08
Al	5.50	5.55	5.67	5.42	5.64	5.65	5.40
Zr	0.05	0.07	0.05	0.04	0.04	0.05	0.05
B	0.014	0.013	0.014	0.013	0.015	0.014	0.014
Fe	0.09	0.09	0.09	0.09	0.09	0.09	0.09
W	10.20	10.35	10.40	10.40	10.30	10.40	10.15
Ta	3.23	3.28	3.25	3.19	3.30	3.20	3.25
Hf	1.60	1.55	1.50	1.30	1.60	1.60	1.55
Ni	Bal.	Bal.	Bal.	Bal.	Bal.	Bal.	Bal.

*not determined.

ORIGINAL PAGE IS
OF POOR QUALITY

TABLE V. Chemical Composition of Second Pour Castings.

(Weight Percent)

Element	Ingot Number 1	15	30	45	60	75	91
C	0.153	0.150	0.155	0.155	0.153	0.145	0.150
Mn	0.01	0.01	0.02	0.02	0.01	0.010	0.010
S	0.002	0.002	0.002	0.002	0.002	0.002	0.002
P	*	*	*	*	*	*	*
Si	0.05	0.05	0.05	0.05	0.05	0.05	0.05
Cr	8.35	8.38	8.35	8.38	8.35	8.28	8.28
Co	9.94	9.90	9.91	9.90	9.90	9.92	9.91
Mo	0.70	0.69	0.69	0.68	0.67	0.69	0.68
Ti	1.05	1.03	1.05	1.02	1.02	1.00	0.99
Al	5.60	5.57	5.55	5.58	5.56	5.50	5.50
Zr	0.055	0.060	0.055	0.055	0.060	0.05	0.05
B	0.013	0.014	0.013	0.014	0.013	0.013	0.013
Fe	0.09	0.09	0.10	0.00	0.09	0.09	0.09
W	10.05	9.99	10.02	9.97	9.97	9.99	9.97
Ta	2.95	2.93	2.96	2.95	2.97	2.94	2.97
Hf	1.48	1.45	1.45	1.43	1.43	1.45	1.47
Ni	Bal.	Bal.	Bal.	Bal.	Bal.	Bal.	Bal.

*not determined.

ORIGINAL PAGE IS
OF POOR QUALITY

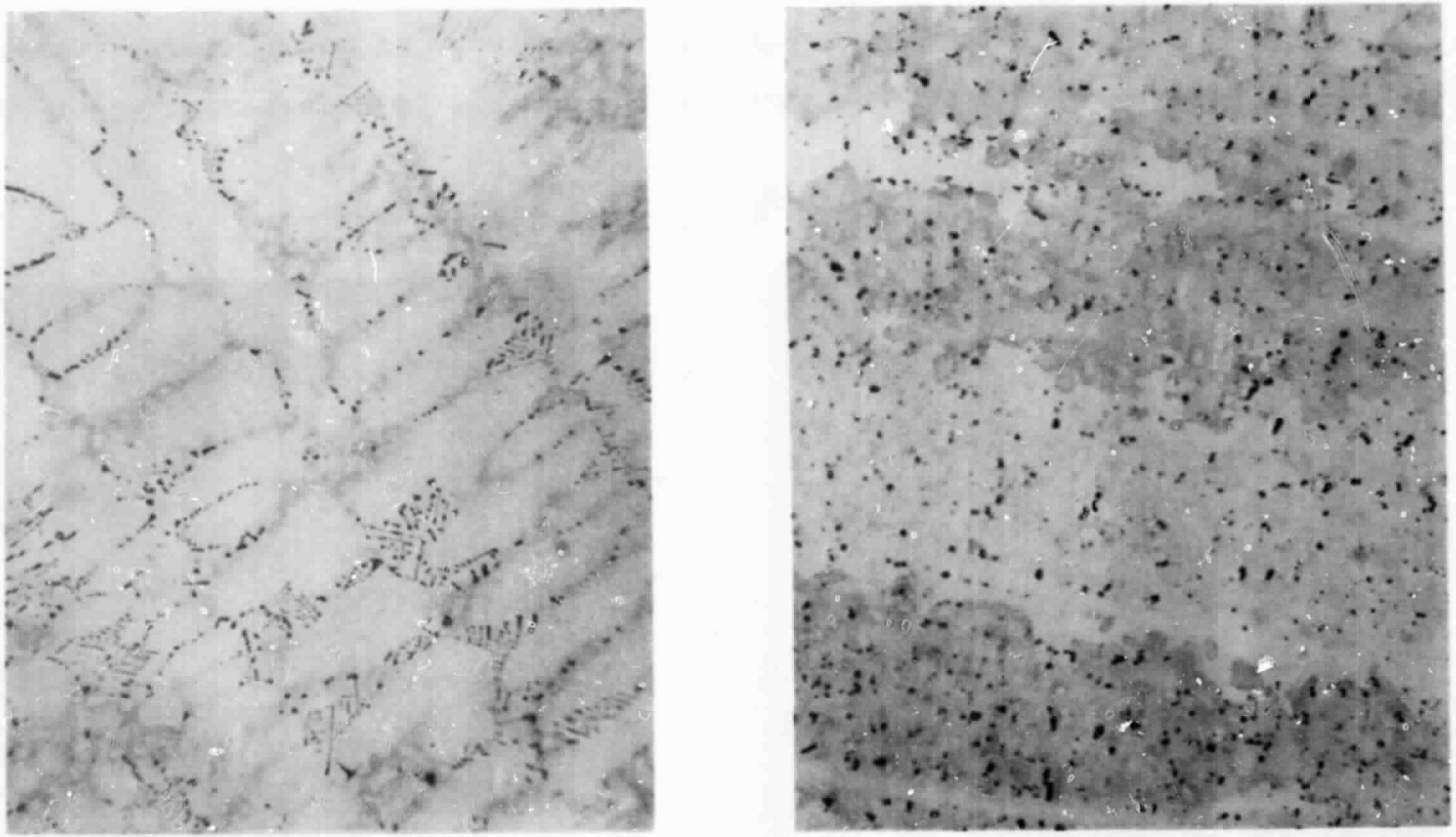

(a) (b)

Fig. 1-Optical micrographs showing the MC carbide distribution at the center (a) and edge (b) of the middle slice of ingot number 99.

ORIGINAL PAGE IS
OF POOR QUALITY

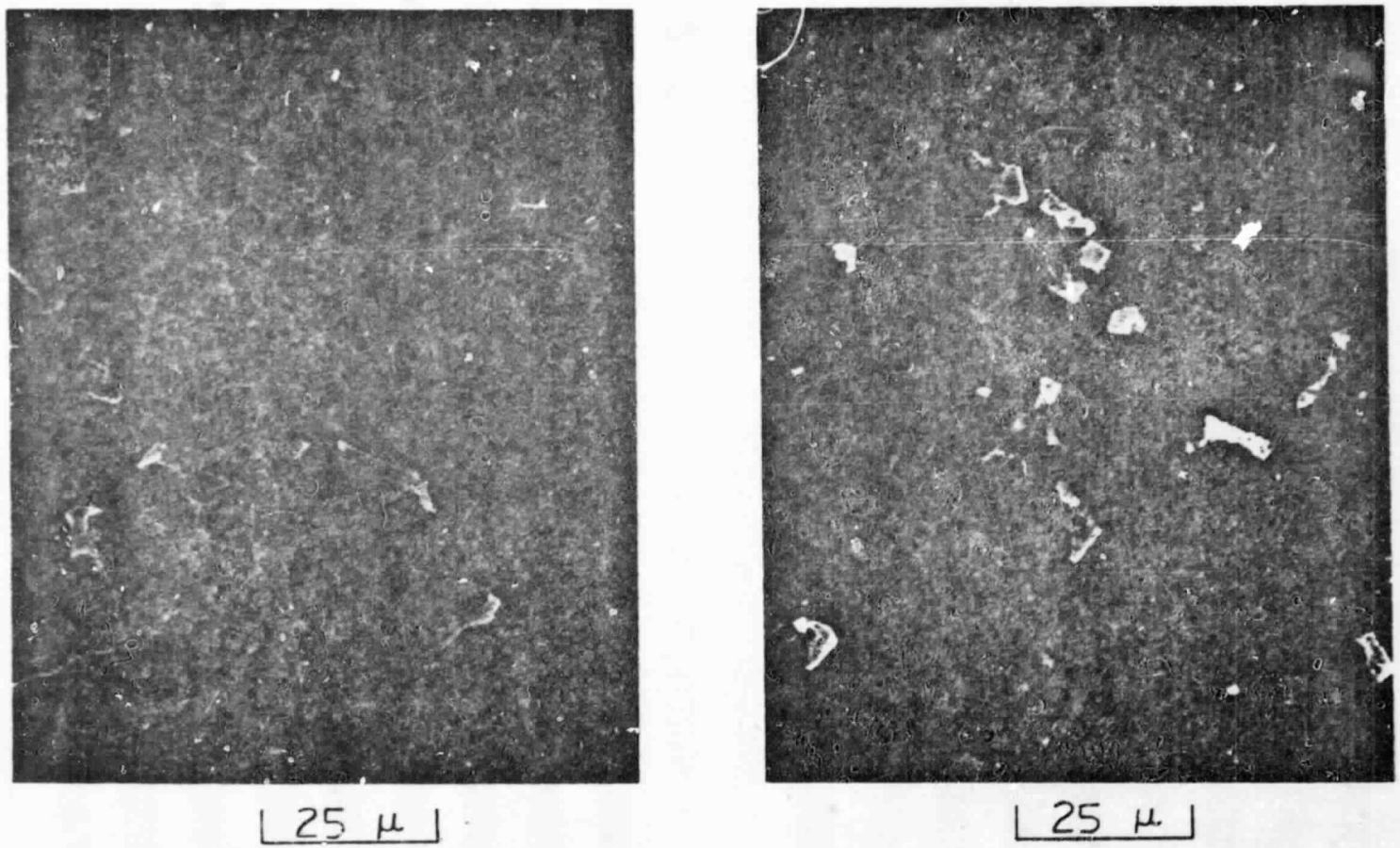

(a) (b)

Fig. 2-SEM micrographs of the center (a) and edge (b) specimens from the middle slice of ingot number 99 showing the MC carbide morphologies.

ORIGINAL PAGE IS
OF POOR QUALITY

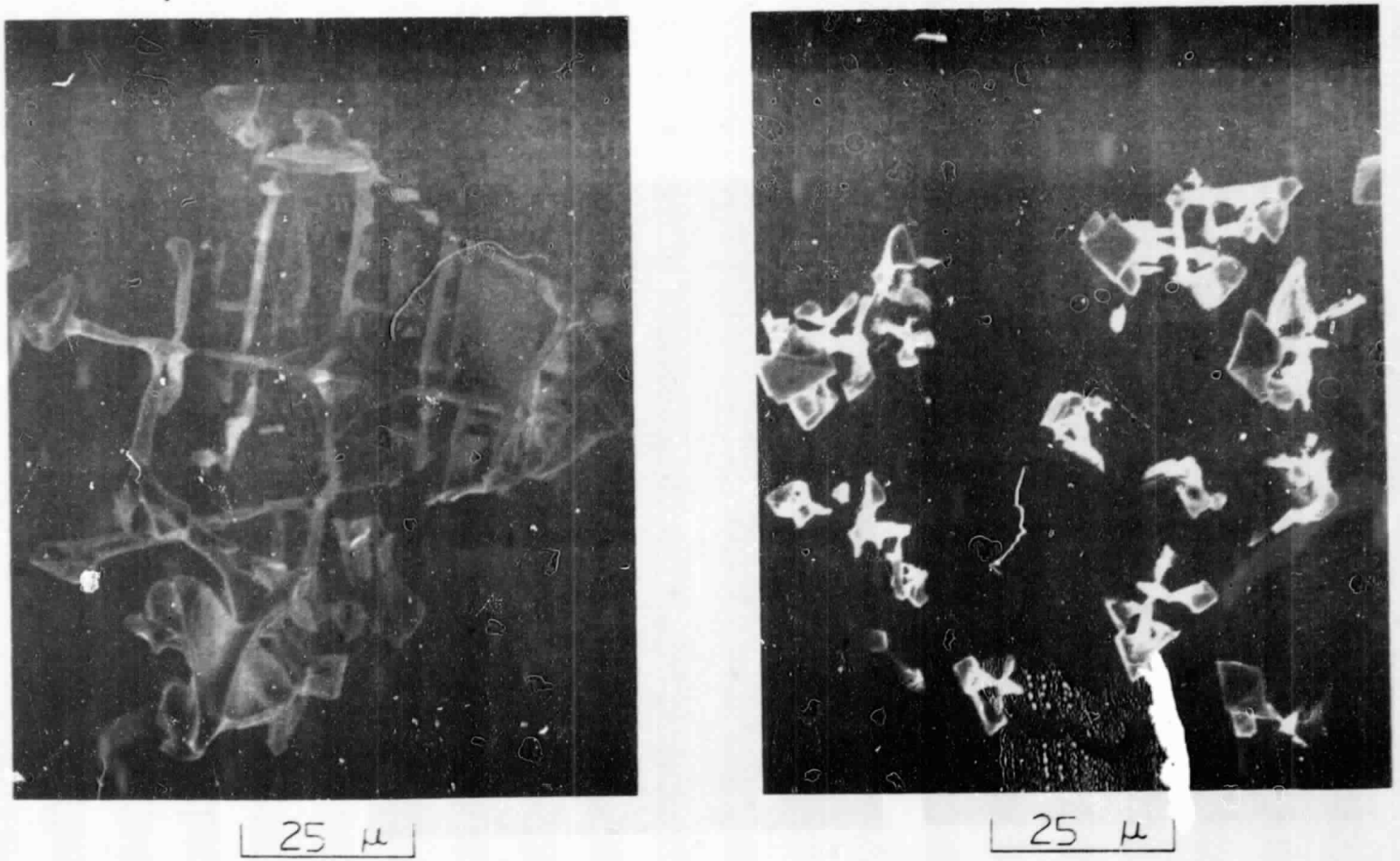

(a) (b)

Fig. 3-SEM micrographs of deeply electropolished center (a) and edge (b) specimens from the middle slice of ingot number 99 showing MC carbide script structures.

ORIGINAL PAGE IS
OF POOR QUALITY

ORIGINAL PAGE IS
OF POOR QUALITY

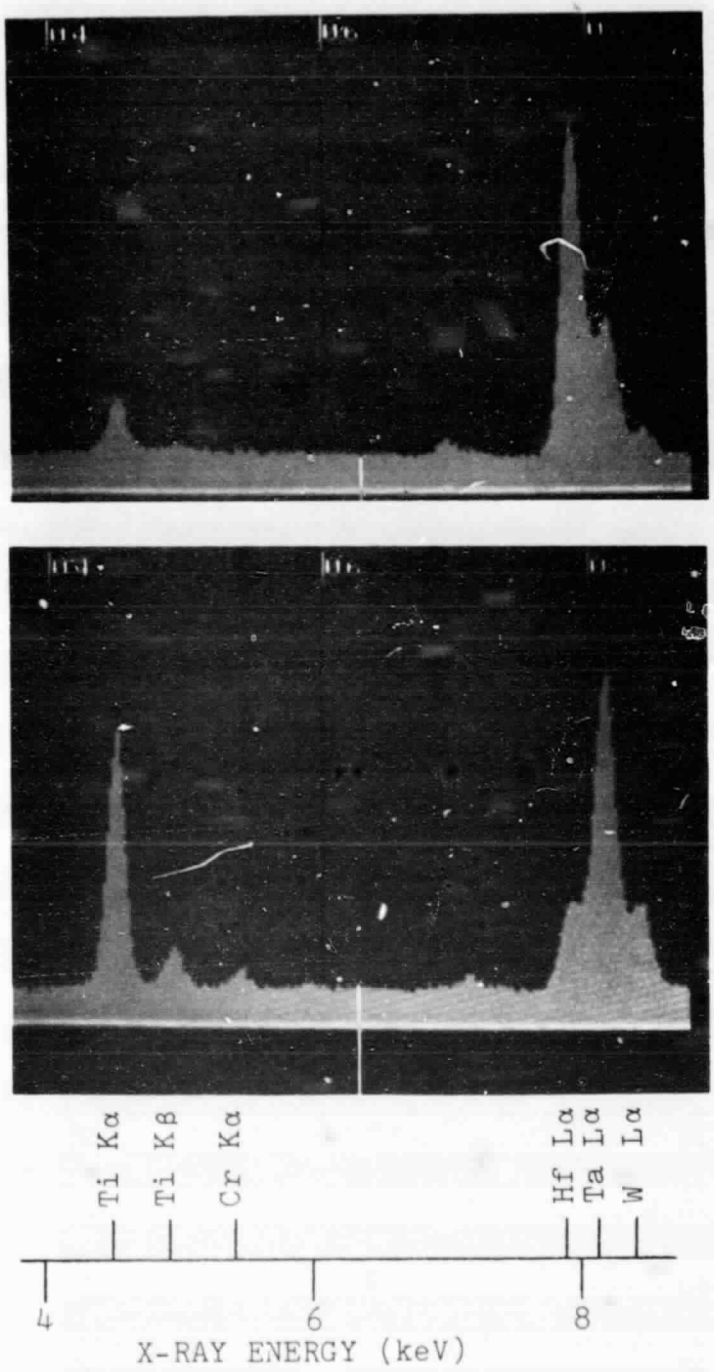

Fig. 4- Energy-dispersive x-ray spectra from extracted MC carbides: (a) is typical of the "head" portions of the script carbides, (b) is typical of the "core" and "arm" portions.

ORIGINAL PAGE IS
OF POOR QUALITY

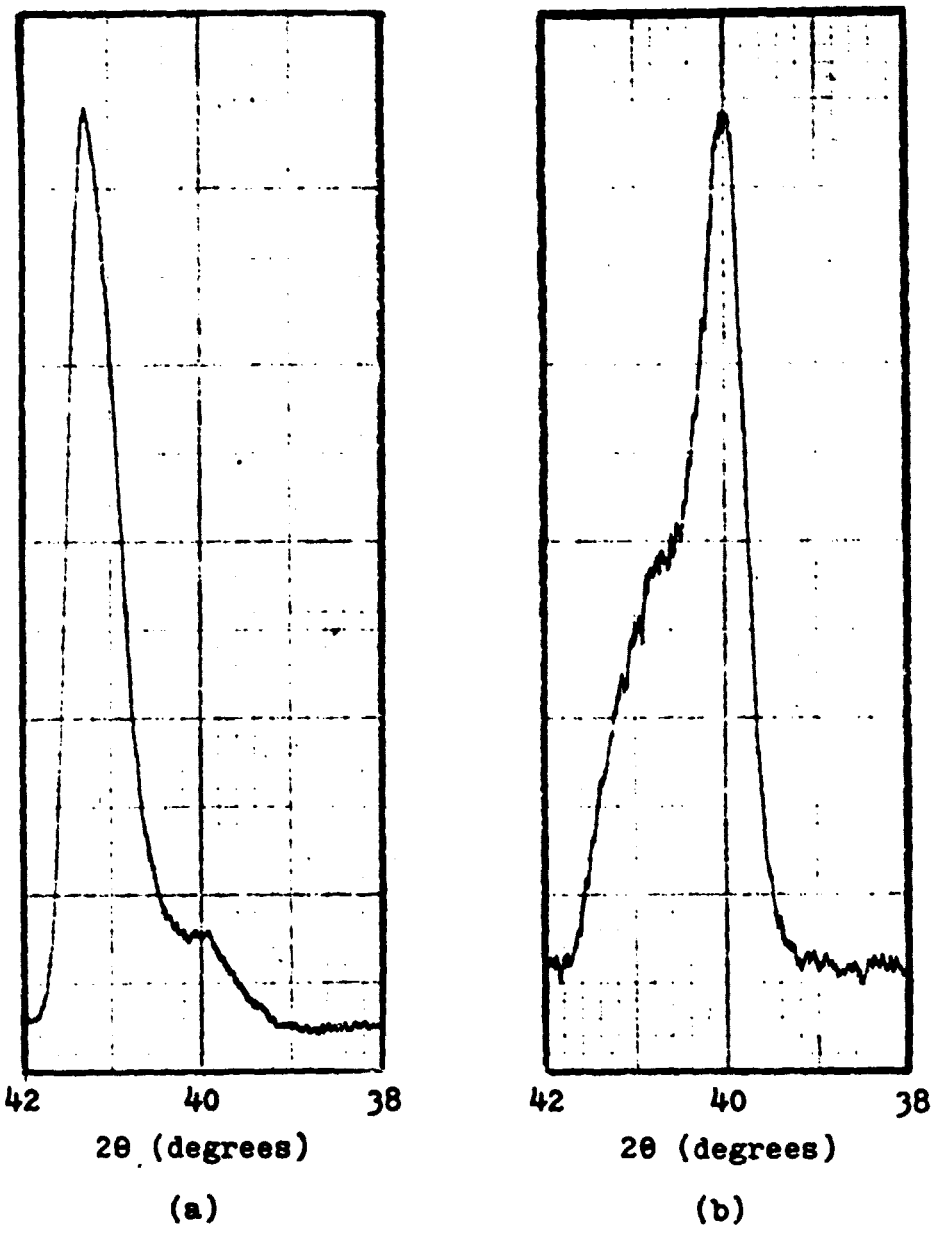

Fig. 5- X-ray diffraction profiles of MC carbide (200) peaks extracted from the middle slice of ingot number 99: (a) is from the center of the ingot, and (b) is from the outer edge of the ingot.

ORIGINAL PAGE
BLACK AND WHITE PHOTOGRAPH

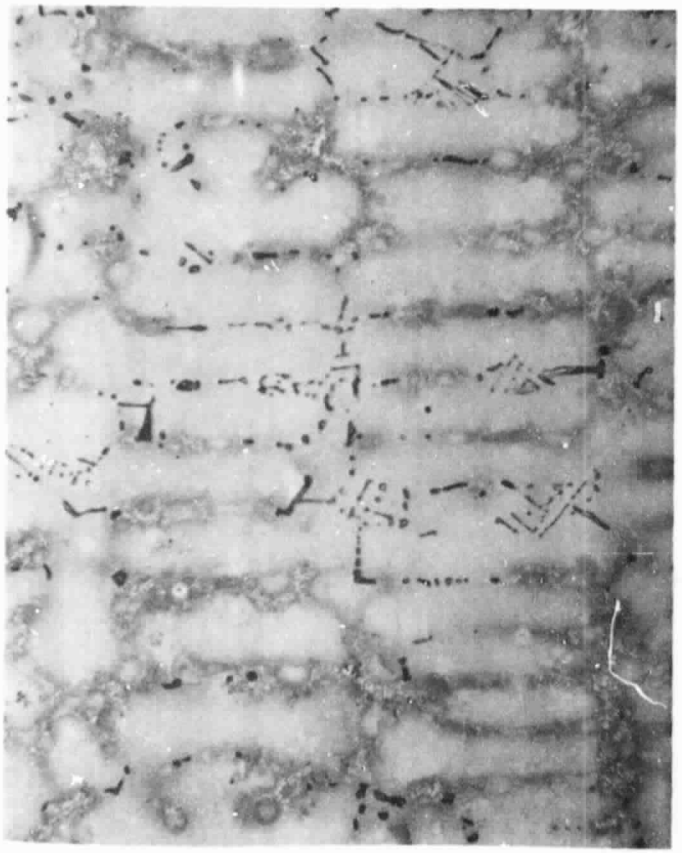

Fig. 7-Optical micrograph of gating center showing MC carbide distribution.

Fig. 8-SEM micrograph of gating center showing script MC carbide.

ORIGINAL PAGE
BLACK AND WHITE PHOTOGRAPH

Fig. 9-SEM micrographs of the root section of blade number 2 showing script MC carbide (a), and grain boundary $M_{23}C_6$ (b).

ORIGINAL PAGE
BLACK AND WHITE PHOTOGRAPH

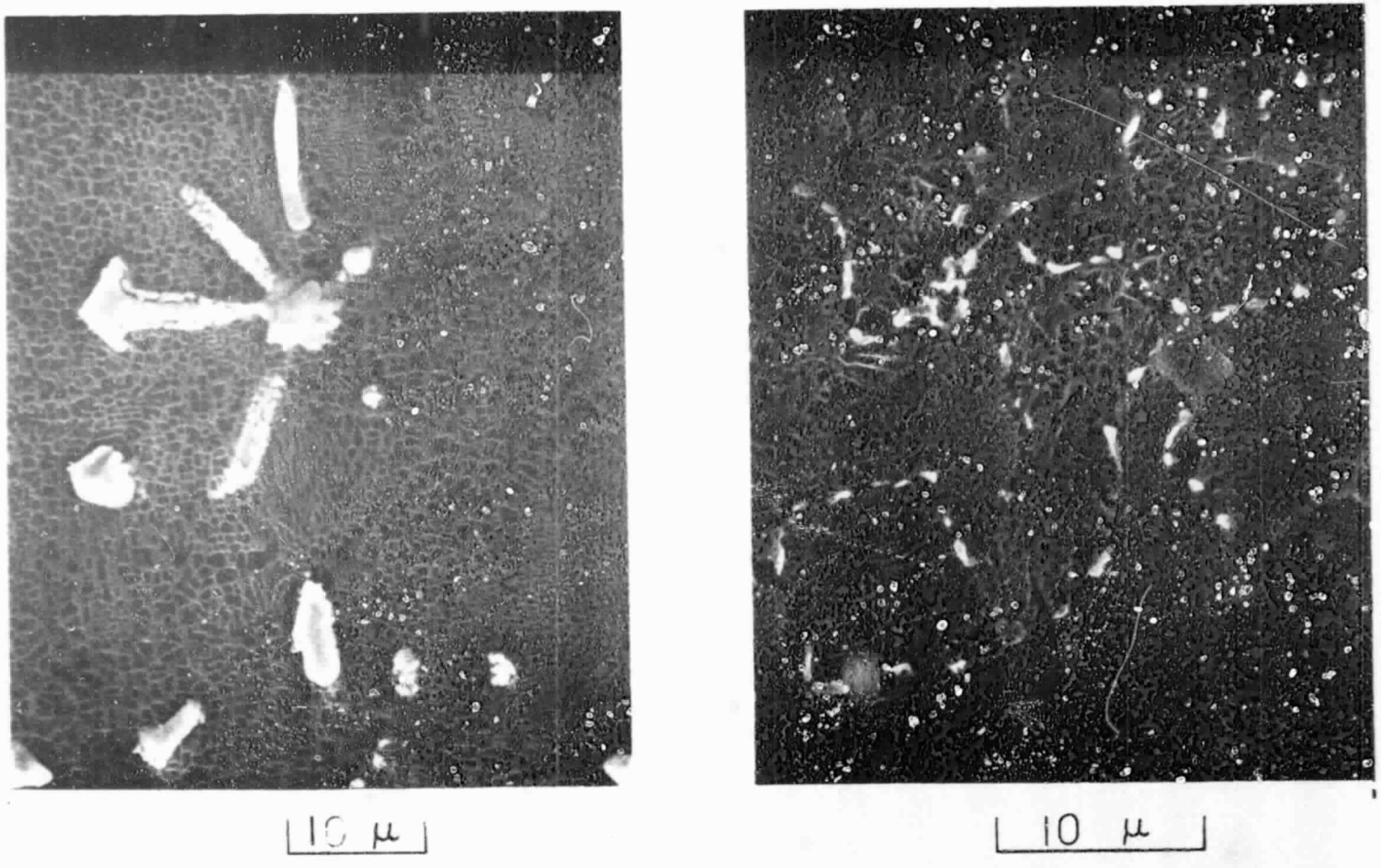

(a) (b)

Fig. 10-SEM micrographs of the airfoil section of blade number 2 showing MC carbide (a), and discrete $M_{23}C_6$ at the edges of primary γ' islands (b).

ORIGINAL PAGE
BLACK AND WHITE PHOTOGRAPH

Fig. 11-SEM micrographs of deeply electropolished gating (a) and root (b) specimens showing MC carbide script structures.

ORIGINAL PAGE
BLACK AND WHITE PHOTOGRAPH

Fig. 12-SEM micrographs of deeply electropolished airfoil specimen showing fine MC carbide script structures at two different magnifications.

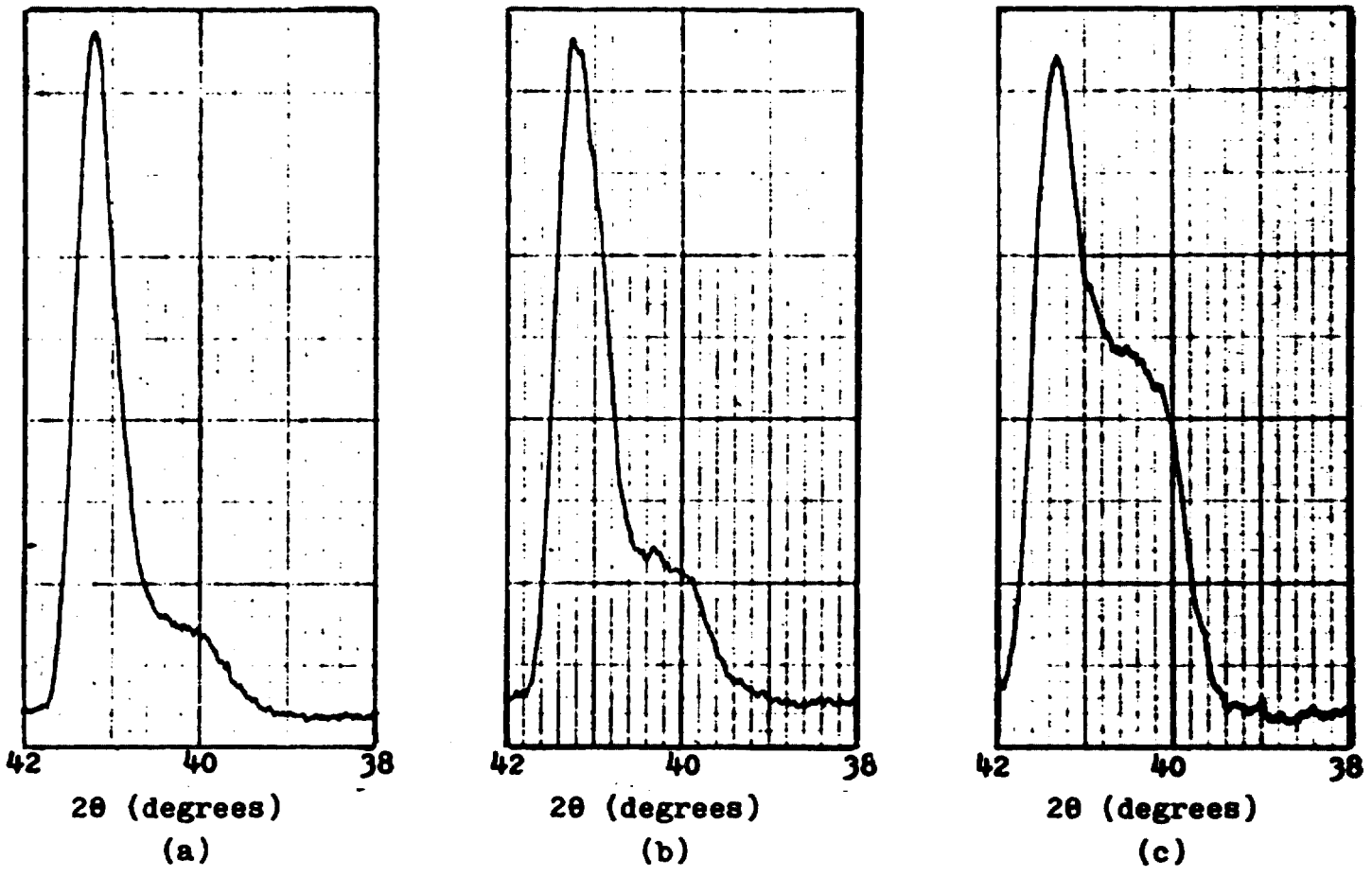

Fig. 13- X-ray diffraction profiles of MC carbide (200) peaks extracted from the castings: (a) is typical of the center of the gatings, (b) is typical of the blade root sections, and (c) is typical of the blade airfoil sections.

ORIGINAL PAGE IS
OF POOR QUALITY